KORDI program for typhoon-ocean interaction in the shelf seas and Northwestern Pacific

S.K. Kang[a*], H.W. Kang[a], Y.H. Kim[a], J.K. So[a], J.H. Lee[a], H.J. lie[a], S.W. Yeh[a], E.J. Kim[a], O.H. Seo[a], I. Ginis[b]
[a] Korea Ocean Research & Development Institute, Ansan, Seoul, Korea
[b] University of Rhode Island, USA

1. Introduction

A research program for ocean-typhoon coupling in the Korean marginal seas and Northwestern Pacific has been launched. The program also aims at understanding the ocean response under typhoon pass in the shelf region of the East China Sea where typhoon weakens due to low ocean heat content, and the Kuroshio region where typhoon intensifies due to high ocean heat content. The coupling of ocean and typhoon models is also investigated for the Northwestern pacific region. One of the major goals is to set up the accurate typhoon prediction system under ocean-typhoon coupling, based upon the initialization of observed data. KORDI and URI cooperate for the coupling of the ocean and typhoon models.

2. Field program in summer 2007

2.1 Field surveys before and after typhoon Nari

Field program in the Yellow and East China shelf seas for understanding ocean process has been carried out during summer and autumn, 2007, shown in Fig. 2.1. Temperature and salinity through CTD casting have been measured, before (27~31Aug.) and after (17~21Sep.) the typhoon Nari passed across the East China Sea toward Korean peninsula, while ocean drifters as well as ADCP have been deployed during the 1st field work (27~31Aug.) and ADCP was recovered after one month mooring, as marked in Fig. 2.1.

About 15 days after 1st CTD casting (27~31Aug.) typhoon passed through ECS. Typhoon Nari was developed as tropical storm on 05:00, Sep. 14 (KST), according to JTWC message data, intensified up to category 4 while it pass through Kuroshio Current north of Ryukyu island, and landed on Korean peninsula on Sep. 17.

---

* *Corresponding author address* : Kang Sok Kuh, KORDI, Ansan P.O. Box 29, Seoul 425-600, Korea; e-mail:skkang@kordi.re.kr

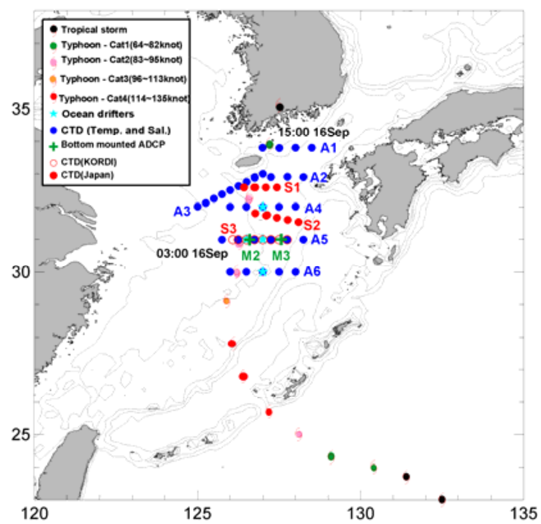

Fig.2.1 Field observation before and after typhoon Nari's passage. Stations for CTD (temp. and sal.) casting and surface drifter release with temperature sensors are noted, along with ADCP stations(M2, M3).

Fortunately just two days after Nari's passage temperature and salinity (sections S1~S2) were measured and also done 15 days after typhoon passed.

Figure 2.2 shows the vertical temperature sections 15 days (A5) before and 2 days (S2) after typhoon Nari's passage, as well as 15 days (S3) after typhoon's passage. The isothermal lines before typhoon (a) are relatively parallel with depths and the depth of 26℃ reaches down to 20m ant western section while 26℃ down to 50m depth at shelf slope region. Even 29.5℃ Contour is also found in the upper layer. Two days after typhoon the temperature structure (A2) shows abrupt change, with 25-27℃ isothermal lines outcropped to the sea surface due to upwelling or mixing by typhoon. Point of surface outcropping appears around 50 to 100 km right of typhoon track and more accurate estimation for the distance between surface crossing point and typhoon track may be renewable when best track data is available later.

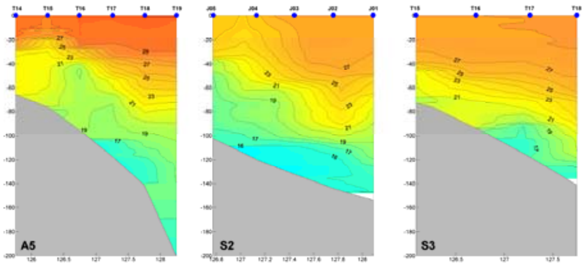

Fig.2.2 Vertical temperature structures, 15 days before (Section A5), 2 days after (Sectione S2), 15 days after (section S3) typhoon's passage.

The ocean heat content (OHC) was also computed using the measured data, as shown in Fig. 2.3a. OHC reaches up to 56 KJ/cm² (13,300 cal/cm²), while minimum OHC goes down to 0 KJ/cm², as shown in inset, since 26℃ isothermal line is not seen in the western station of section S2, after typhoon's passage.

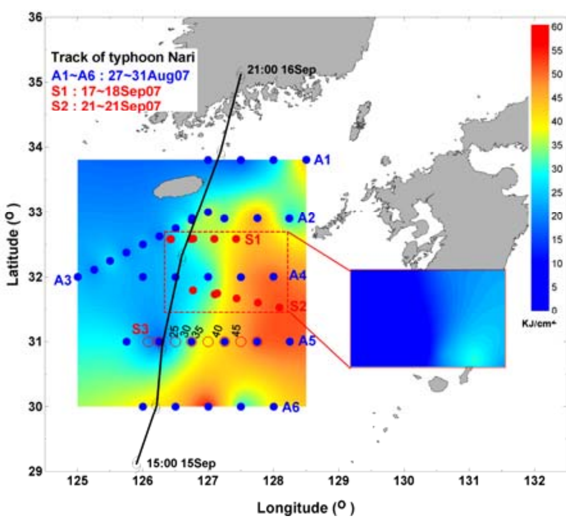

Fig.2.3a Spatial pattern of cean heat content (OHC) 15 days before (A stations) and 2 days after (S1 and S2 stations) typhoon Nari's passage.

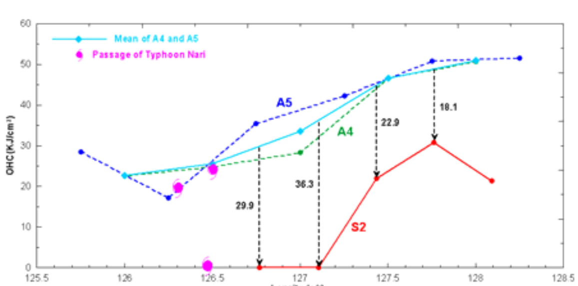

Fig.2.3b Ocean heat content comparison between mean of (A4 and A5) and S2. Circles with tails denote the crossing latitude of the typhoon track, as seen in Fig 2.3a.

Obvious contrast of OHC is seen in Fig.2.3b, as evidenced from the comparison of mean (A4 and A5) and S2. It is clearly seen that ocean heat energy is greatly decreased, after typhoon's passing. Peak heat energy drain in the section S2 after typhoon passage is about 36.3 KJ/cm² (8642 cal/cm²).

It is interesting to note that the remaining OHC after typhoon's passage is actually zero in the nearest western two stations of S2 in typhoon track. The distance from typhoon track with zero OHC is occupied over the region from 25km (126.7ºE) to 56km (127.1ºE). Therefore, maximum drain of OHC at section S2 occurs around 50km distance from typhoon track.

2.2 Data using bottom mounted ADCP and drifting buoys

As shown in Fig.1, two ADCPs (M2 and M3) each with four beams are located about 20km apart (M2) from the track and about 115km apart (M3), and 10 minute averaged velocity component were measured, as well as echo intensity and every 20 minute wave data per every 3 hours. It is interesting to note that observed vertical velocities around the time of Nari's passage near M2 are quite strong, with larger than 10cm/s, and short period oscillation looks dominated, as presented in Fig. 2.4a. As mentioned above, typhoon Nari passed through the nearest point of M2 is around 03:00, Sep. 16, when strong negative vertical velocity is dominant over the column even to the bottom.

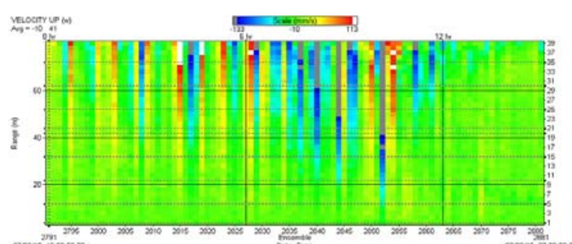

Fig.2.4a Temporal variation of veritical velocity component around the time of typhoon's passing the 30km distance point from M2.

This alternating (+ ande -) vertical velocity is expected to contribute as dynamical mechanism to driving vertical mixing or upwelling of lower layer water. During the nearly same period of high vertical velocity, echo intensity in four beams shows larger values down to surface 30 meter, since water depth is about 90m, as shown Fig.2.4b, while the wave height is large with the peak significant wave height of over 15m. Since data interval for velocity and echo intensity is 10 minute, it is difficult to what process induce such a short period oscillation, even though short waves are expected to be closely associated with the phenomenon.

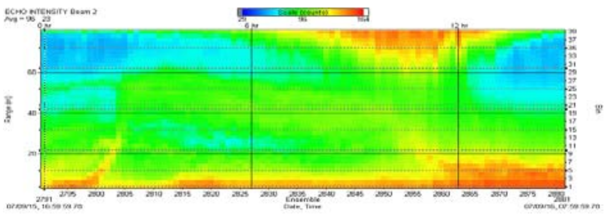

Fig.2.4b Echo intensity of beam2, with similar pattern between four beams around the time of typhoon's passing the 30km distance point from M2.

In relation to the possible error or homogeneity to measure the vertical velocity the angle of each beam and vertical axis is 20º and the distance between two opposing axes is about 60m and homogeneity of velocity component can be argued, even though wave length with period of 10s is about 300m.

From the lagrangian observation of temperature profile before and after typhoon, surface water temperature was decreased by 3.7℃, compared with that before typhoon passage, and cold water mass after the typhoon passed through the region persisted over nearly 10 days or more, which has been verified from surface temperature observed by the deployed drifters with underwater temperature chains.

3. Numerical models

3.1 Ocean circulation models

Ocean models for the Northwestern Pacific are being set up using several types of ocean models, while URI group is developing typhoon model in addition. The relation between the long term variability of typhoon occurrence frequency and SST in tropical Pacific is also examined.

To understand the ocean response and its role to the typhoon as well as to serve as an ocean component for the coupled ocean and atmosphere typhoon prediction system, we developed two kinds of ocean model in the region of Northwestern Pacific focusing around the Korean Peninsula. One is a high (1/12 degree) resolution model based on the MOM3 (Modular Ocean Model version 3, Pacanowski and Griffies, 1999) and the other is a medium (1/4 degree) resolution model based on the HYCOM (HYbrid Coordinate Ocean Model, Bleck, 2002). The medium resolution model covers most of the East Asian Marginal Seas (105E ~ 170E, 10N ~ 65N, thus we call this EAMS1/4 hereafter) and the high resolution model focuses on the typhoon passages to the Korean Peninsula covering 115E ~ 150E, 15N ~ 52N.

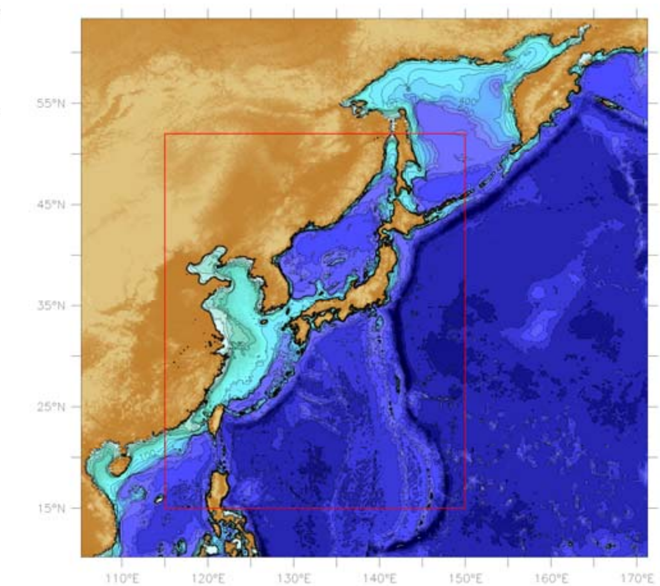

Fig. 3.1 Domain of medium range of ocean circulation model and the bathymetry. The red box shows the high resolution model domain.

3.1.1 EAMS1/4

We set up the HYCOM in the area of East Asian Marginal Seas with a quarter degree resolution. The HYCOM by Bleck (2002) is an outgrowth of the MICOM (Miami Isopycnal Coordinate Ocean Model, Bleck and Smith, 1990). The major improvements in HYCOM relative to MICOM is the introduction of a hybrid vertical coordinate, which allows for the use of coordinate formulations suitable for different ocean regimes. The hybrid coordinate is typically isopycnal in the open, stratified ocean, but there is a smooth transition to z-level coordinates in the mixed layer and a transition to sigma coordinates in shallow coastal regions. This approach allows for high vertical resolution close to the surface and in shallow regions, and has also allowed for implementation of non-slab vertical mixing schemes like the K-profile parameterization (KPP; Large et al., 1994). Seas around Korean Peninsula and the Northwestern Pacific have very complex topography including continental shelf less than 100m and world's deepest trench as shown by Fig. 3.1., which is the best candidate for the HYCOM application.

EAMS1/4 model has been developed for now and is under testing stage for the simulation of the thermal structure of the upper Northwestern Pacific ocean and the continental shelf region in the Yellow Sea and the East China Sea. The initial condition is the January climatological temperature and salinity with no motion derived from the Levitus climatology data. The lateral boundary conditions are imposed to the southern and eastern boundaries (Fig. 3.2) by the nesting method. The physical and dynamical variables at the open boundaries are estimated from 50 year spun-up results of the low resolution global ocean model which has been concurrently carried on for this study. In both models, forcings at the sea surface are adopted from the COADS (Comprehensive Ocean-Atmosphere Data Set) climatology. The following results of the EAMS1/4 are those of the 7 years spin-up after nesting.

Figures 3.2 and 3.3 show well the seasonal contrast of the sea surface temperature (SST) and the vertical thermal structure at the meridional section of 125 E. In Fig. 3.2, the major current system such as North Equatorial Current (NEC), Kuroshio Current and its extension is well simulated. It is shown that the SST in August is more than 30 ℃ in most of the southern region. On the contrary, the SST in the February is about 21 ℃ to the north of the 20 N.

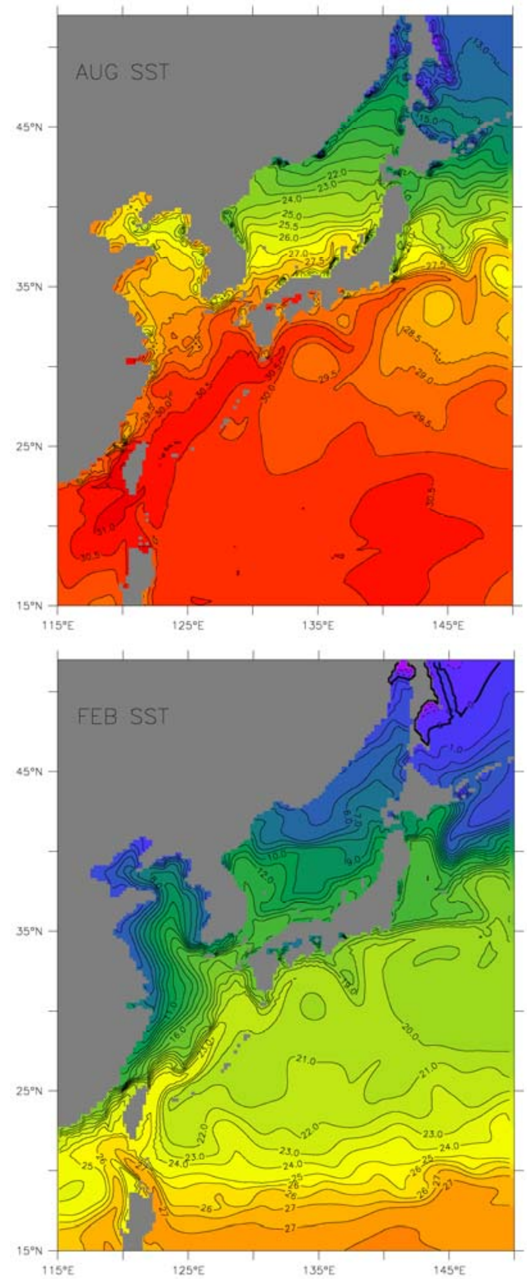

Fig. 3.2 Sea surface temperature in February and August.

Fig. 3.3 shows the contrast of the vertical thermal structure at the section of 125E. In summer, it is noteworthy that the stratification is enhanced, especially in the continental shelf region of the East China Sea and the Yellow Sea. In winter, those structures of the strong thermal stratification collapsed and most of the water in the shelf region seems to be well mixed. In the offshore or Pacific region, both of the NEC and the Kuroshio comprising the subtropical gyre have been intensified in summer.

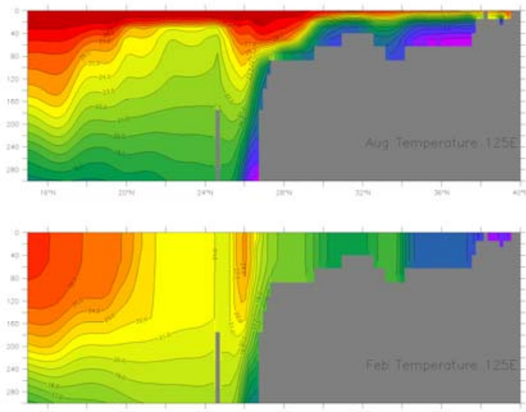

Fig. 3.3 Vertical thermal structure shown by the temperature at the section of125E (Left : Aug. Right: Feb.)

Before moving to the coupling with the typhoon model, we have carried on a simple experiment on the oceanic response to the typhoon. An ideal axis symmetric typhoon which radius is about 300 km with the constant moving speed has been generated in the southern part of the model domain. It has passed through the Northwestern Pacific heading northward as in the Fig. 3.4. It is noticeable that the sea surface temperature has been decreased about 3 ~ 4 ℃ in the right the right pane of the Fig. 3.4.

.

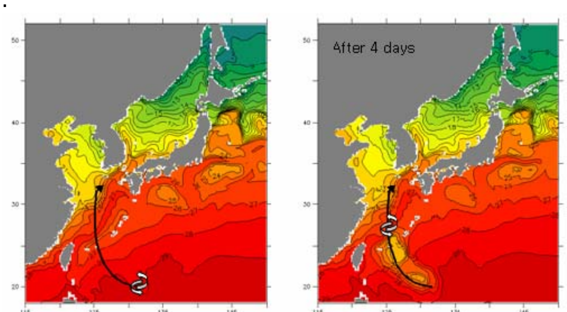

Fig. 3.4 Ocean response to the simple artificial typhoon passing

It is planned that fully coupling with the GFDL (Geophysical Fluid Dynamics Laboratory) typhoon model in the near future. In addition, coupling with the simple typhoon intensity model for the process study will be carried on. It is expected that this effort for the development of the coupled typhoon prediction system could contribute to the regional typhoon damage as well as the improvement of the prediction accuracy.

3.1.2 MOM1/12

We have developed a data assimilative regional ocean model in the northwestern Pacific based on the MOM 3 which is a finite difference model with the horizontal B-grid and vertical z-coordinate. The model domain is from 115°E to 150°E and from 15°N to 52°N with 1/12° horizontal resolution. The numbers of the longitudinal and latitudinal grids are 420 and 444, respectively. To resolve the bottom geometry more accurately, the partial bottom cell scheme was used (Pacanowski and Gnanadesikan, 1998) and high resolution bathymetry of 1/60° (Choi et al., 2002) and ETOPO2 bathymetry were adopted for the model topography (Fig. 1). The vertical resolution is varying from 10 m at the surface to about 700 m at the bottom with 35 vertical levels. The momentum equation has been split into the barotropic and baroclinic modes. The model was initialized using hydrographic data from WOA (World Ocean Atlas, 2002), and forced by monthly mean surface and open boundary conditions. Surface windstress, heat flux are given from the NCEP meteorological datasets and for the salt flux, the surface salinity in the model is relaxed to that of the WOA. A radiation condition with a nudging term is applied to the tracers and barotropic current from the HYCOM Consortium data products along the open boundary (Marchesiello et al., 2001).

The 3-dimensional variational assimilation routine has been fully coupled with the regional ocean model, and temperature profiles, and satellite-borne sea surface temperature and surface height have been assimilated following Weaver and Courtier (2001). Among several different methods to assimilate the sea surface height (SSH) into ocean models, we followed Cooper and Haines (1996). Their method is to rearrange preexisting water masses under an assumption of conservation of water properties and potential vorticity. The simple way of Cooper and Haines (1996) to satisfy the conservation assumptions is to displace water columns so that the change in the surface pressure should be compensated by the change in weight of the entire water columns.

Fig. 3.5 shows preliminary results of the MOM1/12 without data assimilation. The model has been forced by the climatological monthly mean windstress, heat and salt flux. The major current system such as Kuroshio Current and its extension is well simulated while the Kuroshio Current tends to overshoot.

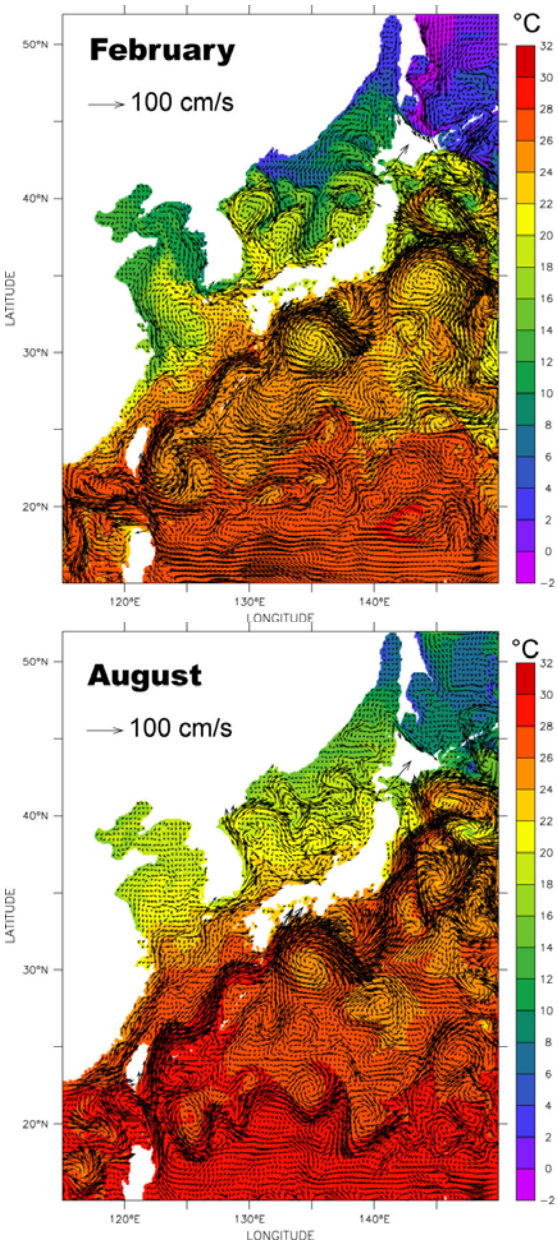

Fig. 3.5. Sea surface temperature and current in February and August from the MOM1/12 without data assimilation.

3.1.3 ESCORT model

We are going to also apply ESCORT (Efficient Support for Coastal and Ocean Research and Test) system for the typhoon-ocean interaction, which is a full three-dimensional ocean model and a kind of modular model comprising Eulerian transport and Lagrangian particle tracking module for computation of scalar transport developed by KORDI. This model system uses finite difference method in space. Several options for σ-coordinate, z-coordinate or hybrid coordinate in vertical are prepared and s-coordinate option will be included in the near future. Partial bottom cell can be adopted to reflect more realistic bottom topography in case of z- or hybrid vertical coordinate. Mode splitting technique that momentum equations are splitted into external and internal mode is applied for economy. Leapfrog time-stepping and TVD(Total Variance Diminishing) advection scheme are major features of this model. Equations are solved explicitly in horizontal plain but vertical diffusion equations are solved implicitly for numerical stability. Eddy viscosity/diffusivity are computed mainly by Smagorinsky formula. A stable dry/wet method is applied at the tidal-flat cells and relay-start is possible against an abrupt halt.

3.2 Typhoon model

The typhoon model is based on the Geophysical Fluid Dynamics Laboratory (GFDL) hurricane prediction system that became operational in 1995 as the U.S. National Weather Service's (NWS) official hurricane model (Bender et al. 2007). Since that time, it has provided forecast guidance to forecasters at the NWS's Tropical Prediction Center (TPC). Overall, the GFDL system has been the most reliable model for track forecasts during the past decade and has made a significant contribution toward reducing the official track error. A version of the GFDL model (GFDN) was transferred to the United States Navy in 1996 to provide forecast guidance in the Western Pacific. At present the GFDL model is applied for tropical cyclones globally. Over the years numerous improvements to the model physics and the model's horizontal and vertical resolution have been made. The most recent improvements are described in Bender et al. (2007). These include the transition of the GFDL model from an uncoupled atmospheric model to a coupled atmosphere-ocean model with a fully interactive ocean. Previous studies (Bender and Ginis 2000) confirmed the importance of the ocean coupling to intensity prediction with the GFDL hurricane model, particularly for slower moving storms. In 2003 the GFDL model's vertical levels were increased from 18 to 42 sigma levels and its cumulus parameterization and boundary layer physics were replaced with the physics packages operational in NCEP's global model (GFS). This resulted in the lowest track errors ever for the GFDL model in that year, with a 72-hour error of only 137 nautical miles (nm). Two years later, the model's finest resolution was doubled to onetwelfth degree in time for the 2005 record-breaking Atlantic hurricane season. In the 2006 physics upgrade NCEP's Ferrier cloud-microphysics package was introduced along with an improved air-sea momentum flux parameterization developed at URI. These major physics upgrades have resulted in very significant improvements in intensity prediction. The overall reduction in the GFDL errors in 2006 was nearly 33% compared to its performance over the past 6 years.

4. Summary

The first year activities on the KORDI program for typhoon-ocean interaction in the Northwestern Pacific have been briefly described. The first observation has been focused on the East China Sea. In this summer, we will move to the further southern region around Ryukyu islands where typhoon is usually reinforced with warm ocean water mass (Fig.4.1). Development and validation of coupled ocean-typhoon model will be carried out.

Acknowledgement

This work is supported by KORDI research program (PG46000).

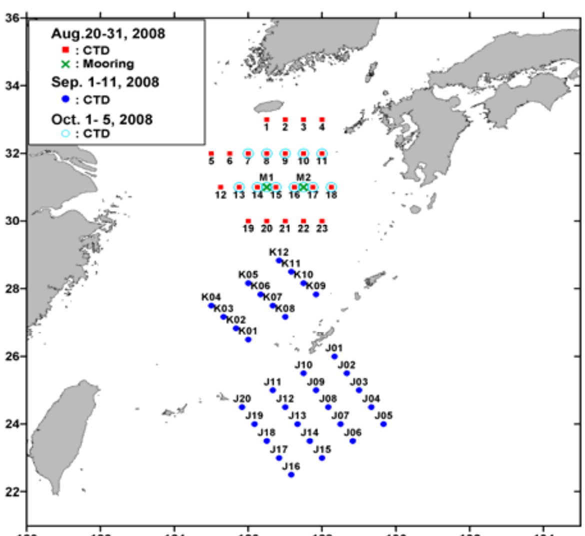

Fig. 4.1 Proposed observation stations during this summer field program. Revised Argo releasing point and surface drifter points are not marked.

5. References

Bender, M.A., I. Ginis, R. Tuleya, B. Thomas, T. Marchok, 2007: The operational GFDL coupled hurricane-ocean prediction system and a summary of its performance. *Mon. Wea. Rev*. 135, 3965-3989.

Bender, M.A. and I. Ginis, 2000: Real-case simulations of hurricane-ocean interaction using a high-resolution coupled model: Effects on hurricane intensity. *Mon. Wea. Rev*., 128, 917-946.

Bleck, R., 2002, An oceanic general circulation model framed in hybrid isopycnic-cartesian coordinates. Ocean Model. 4, 55-88.

Bleck, R. and L. T. Smith, 1990, A wind-driven isopycnic coordinate model of the north and equatorial atlantic ocean. 1. Model development and supporting experiments. J. Geophys. Res. 95, 3273-3285.

Choi, B. H., Kim, K. O., Eum, H. M., 2002. Digital bathymetric and topographic data for neighboring seas of Korea. J. Korean Soc. Coastal Ocean Eng., 14, 41–50 (in Korean with English abstract).

Cooper, M., Haines, K., 1996. Altimetric assimilation with water property conservation. J. Geophys. Res., 101(C1), 1959-1977.

Large, W. G., McWilliams, J.C., Doney, S.C., 1994. Oceanic vertical mixing: a review and a model with a nonlocal boundary layer parameterization. Rev. Geophys. 32, 363-403.

Marchesiello, P., McWilliams, J.C., Shchepetkin, A., 2001. Open boundary conditions for long-term integration of regional oceanic models. Ocean Model., 3, 1-20.

Pacanowski, R. C., Griffies, S.M., 1999. MOM3.0 Manual. WWW Page, http://www.gfdl.noaa.gov/~smg/MOM/web/guide_parent/guide_parent.html.

Weaver, A. Courtier, P., 2001. Correlation modeling on the sphere using a generalizing diffusion equation. Q. J. R. Meteorol. Soc., 127, 1815-1846.